Article

Journal of
Nanoscience and Nanotechnology
Vol. 15, 3944–3950, 2015
www.aspbs.com/jnn

Observation of Room Temperature Photoluminescence from Asymmetric $CuGaO_2$/ZnO/ZnMgO Multiple Quantum Well Structures

P. M. Aneesh[1,†], M. K. Jayaraj[1,*], R. Reshmi[1], R. S. Ajimsha[1,‡], L. M. Kukreja[2], A. Aldrin[3§], F. Rojas[3], J. Bertomeu[3], J. López-Vidrier[4], and S. Hernández[4]

[1] *Optoelectronic Devices Laboratory, Department of Physics, Cochin University of Science and Technology, Kochi 682022, India*
[2] *Laser Materials Processing Division, Raja Ramanna Centre for Advanced Technology, Indore 452013, India*
[3] *Departament de Física Aplicada i Òptica, Universitat de Barcelona, Martí i Franquès, 1-11, 5a Planta, 08028-Barcelona, Spain*
[4] *MIND-IN2 UB, Departament d'Electrònica, Universitat de Barcelona Martí i Franquès, 1-11, 2a Planta, 08028-Barcelona, Spain*

Asymmetric ($CuGaO_2$/ZnO/ZnMgO) and symmetric (ZnMgO/ZnO/ZnMgO) multiple quantum well (MQW) structures were successfully fabricated using pulsed laser deposition (PLD) and their comparison were made. Efficient room temperature photoluminescent (PL) emission was observed from these MQWs and temperature dependent luminescence of asymmetric and symmetric MQWs can be explained using the existing theories. A systematic blue shift was observed in both MQWs with decrease in the confinement layer thickness which could be attributed to the quantum confinement effects. The PL emission from asymmetric and symmetric MQW structures were blue shifted compared to 150 nm thick ZnO thin film grown by PLD due to quantum confinement effects.

Keywords: Asymmetric Multiple Quantum Well Structures, Symmetric Multiple Quantum Well Structures ZnO, Pulsed Laser Ablation, Photoluminescence.

1. INTRODUCTION

The optical characteristics of bulk semiconductor materials are determined mainly by the inherent band structure of the material, whereas in the case of quantum well structures the carrier motion is restricted to quasi-two-dimensions, and the confinement of carriers at the nanometer scale gives rise to various quantum effects in the optical properties. Surface recombination is less important in QW structures compared to bulk material. Together with high thermal conductivity, high luminous efficiency and mechanical and chemical robustness, ZnO and its alloys have great prospects in optoelectronics applications in the wavelength range from ultraviolet to the red.[1] Moreover, excitons in ZnO-based quantum well (QW) heterostructures exhibit high stability compared to bulk semiconductors and III–V QWs due to the enhancement in the binding energy[2,3] and the reduction in the exciton-phonon coupling[4] caused by quantum confinement. An important step in order to design high performance ZnO-based optoelectronic devices is the realization of band gap engineering to create barrier layers and quantum wells in heterostructure devices.

Band filling is one of the problems associated with single QW structures which leads to luminescence saturation at high current densities. Multiple quantum well structures consist of more than one well so that more carriers can be injected into the system. Recently, much effort has been devoted towards the investigation and fabrication of symmetric ZnO/ZnMgO multiple quantum wells (MQWs) for UV light emitting applications.[5–9] Ohtomo et al. have grown ZnO/ZnMgO MQWs on lattice mismatched sapphire substrates using laser molecular beam epitaxy, but no photoluminescence (PL) was observed above 150 K.[7,10] In addition, the quantum confinement effects could not be observed in their MQWs through optical absorption spectroscopy,[10] presumably due to the inadequate quality of the grown structures. Krishnamoorthy

*Author to whom correspondence should be addressed.
†Present address: School of Physics, Indian Institute of Science Education and Research (IISER) Trivandrum Campus, Trivandrum 695016, India
‡Present address: Laser Materials Processing Division, Raja Ramanna Centre for Advanced Technology, Indore 452013, India
§Present address: Department of Energy Science and Engineering, Indian Institute of Technology Bombay, Mumbai 400076, India

 1533-4880/2015/15/3944/007 doi:10.1166/jnn.2015.9497

et al.[11] have reported size dependent quantum confinement effects by means of pulsed PL measurements at 77 K in ZnO/ZnMgO single quantum wells grown on sapphire substrates using the pulsed laser deposition. However, a significant improvement in the structural and optical characteristics of ZnO MQWs was accomplished when a lattice-matched substrate $ScAlMgO_4$ (SCAM) was used instead of sapphire, which was evident from the efficient photoluminescence[1, 8, 12] and distinct photon absorption features[13] at room temperature. But the $ScAlMgO_4$ substrates are scarce and expensive compared to abundantly available sapphire substrates. It was therefore imperative to improve the method of growing ZnO MQWs on sapphire to the level that one could get efficient room temperature PL for making them versatile.

Even though there are reports on symmetric MQW, asymmetric quantum well heterostructures are relatively a new concept of band gap engineering for semiconductor optoelectronics. Initial conception of the asymmetric multiple quantum well heterostructure lasers was described early in 1989.[14] In recent years, there has been a considerable interest in asymmetric multiple quantum well systems, because of the possibility to fabricate new optical devices based on inter sub band transitions. Asymmetric quantum wells[15] have the advantage that the electron–hole distance and consequently the strength of the electron–hole interaction can be controlled by an electric field applied perpendicular to the layer. Tsuchiya et al. reported the magnetic field dependence of the luminescence energy in GaAs/AlGaAs asymmetric quantum well as a function of applied electric field.[16] But there are no reports of the luminescence emission studies on ZnO based asymmetric quantum well structures.

$CuMO_2$ (M = Ga, Al) are *p*-type transparent conducting oxides of significant interest for transparent electronics.[17, 18] $CuGaO_2$ is a wide band gap semiconductor with a direct band gap of 3.4–3.6 eV, exhibiting *p*-type conductivity. In $CuGaO_2$ structure, layers of A cations which are linearly coordinated to two oxygen atoms, are alternatively stacked between layers of edge shared $B^{3+}O_6$ octahedra oriented perpendicular to *c*-axis. Band structure calculations indicate that there is also an indirect gap at 0.95 eV.[19, 20] The *p*-type conductivity originates from the +1 valence state of the Cu cation within the delafossite structure. At relatively low growth temperatures, the film is a mixture of $CuGaO_2$, Cu_2O and $CuGa_2O_4$. At higher temperatures, the main phase is $CuGaO_2$. One of the challenges in the growth of $CuGaO_2$ thin films is minimizing the formation of secondary phases, in particular Cu_2O and $CuGa_2O_4$, driven by the variable valence states of Cu cations.

In a semiconductor, electrons are not normally in the conduction band, but they can be excited using optical radiation to form exciton pairs, which consist of an electron that is excited into the conduction band and a hole that the electron leaves behind in the valence band. After the creation of an exciton from a photon, if the photon had more energy than required, the excess energy will be released as a phonon (heat). Normally, the ground state energies in each well are degenerate. However, if an electric field is applied across the layers of the MQW, the degeneracy is lost and the potential appears as a slanted step function. In this case, when a photon has more energy than is required to excite an electron, the excess energy can be used to cause the electron to jump to a neighbouring well with a higher potential from the electric field. Similarly, if the photon has less energy than required for the formation of an exciton, it can still form an exciton as long as the electron subsequently jumps to a well with a lower ground state potential. This carrier injection will be more as in the case of asymmetric MQW structures with *p* and *n* type barrier layers than that of the symmetric MQWs.

In this paper, we report the efficient room temperature PL emission from ten-period asymmetric $CuGaO_2$/ZnO/$Zn_{0.9}Mg_{0.1}O$ MQWs grown on Al_2O_3 substrates by pulsed laser deposition (PLD) and it is compared with ten-period symmetric $Zn_{0.9}Mg_{0.1}O$/ZnO/$Zn_{0.9}Mg_{0.1}O$ MQWs grown by PLD. The temperature dependence of the PL emission of the MQWs is also discussed in detail.

2. EXPERIMENTAL DETAILS

Symmetric and asymmetric multiple quantum wells of $Zn_{0.9}Mg_{0.1}O$/ZnO/$Zn_{0.9}Mg_{0.1}O$ and $CuGaO_2$/ZnO/$Zn_{0.9}Mg_{0.1}O$ were deposited by laser ablation of ceramic targets in O_2 atmosphere. Initially, hot pressed targets of ZnO, $Zn_{0.9}Mg_{0.1}O$ and $CuGaO_2$ were prepared. The ZnO target was prepared from the high purity ZnO powder by the sintering at 1300 °C for 5 hours in air. The $Zn_{0.9}Mg_{0.1}O$ target was prepared by sintering the mixture of ZnO and 10 at.% of high purity MgO powder at 1300 °C. Finally, the $CuGaO_2$ target was prepared by solid state reaction of CuO and Ga_2O_3 powder followed by the sintering at 1100 °C in argon atmosphere.

Each target was ablated individually by the fourth harmonic (266 nm) of a pulsed Nd:YAG laser. The duration of the pulses was maintained at 6–7 ns, while its repetition rate was 10 Hz. The laser beam was focused to a spot size of 2 mm on the surface of the target, which was kept in rotation to avoid pitting. All the depositions were done in an O_2 ambient (99.99 % purity) at a constant pressure of 10^{-3} mbar and with constant laser energy of 2 J/cm^2. The target-to-substrate distance was kept at 6 cm and the substrate temperature was 600 °C. Under these conditions, the growth rate was found to be 0.08 nm/s for ZnO, 0.03 nm/s for ZnMgO and 0.06 nm/s for $CuGaO_2$ films.

Previous to the deposition of the QW layers, a ZnO buffer layer of 50 nm was deposited on top of the sapphire (0001) at 700 °C to avoid possible lattice mismatch-induced effects.[5] Later, ten periods of either $CuGaO_2$/ZnO/$Zn_{0.9}Mg_{0.1}O$ or $Zn_{0.9}Mg_{0.1}O$/ZnO/$Zn_{0.9}Mg_{0.1}O$ were deposited at 600 °C. For both type of structures, the

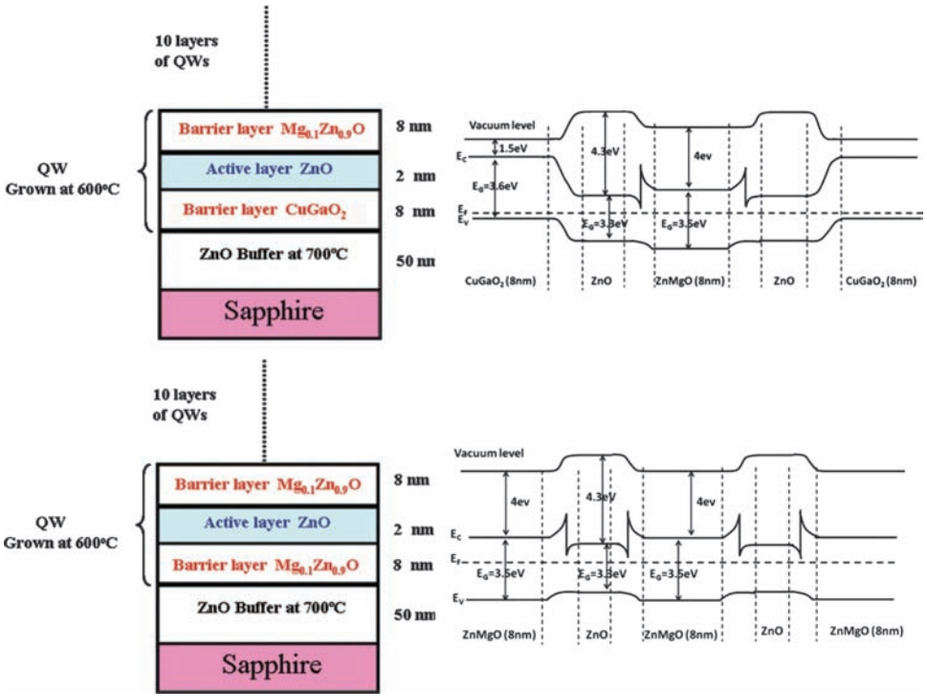

Figure 1. Sample cross-sections and band diagram of the $CuGaO_2$/ZnO/ZnMgO asymmetric (top) and ZnMgO/ZnO/ZnMgO symmetric (bottom) MQW systems grown by PLD.

barrier layers (ZnMgO and $CuGaO_2$) were 8-nm thick, while the ZnO confinement layers presented two nominal thicknesses, either 2 nm or 6 nm. A schematic of the $CuGaO_2$/ZnO/ZnMgO asymmetric MQW and ZnMgO/ZnO/ZnMgO symmetric systems and corresponding band diagrams are shown in Figure 1. Since the valence band of the smaller band gap material (ZnO) lies below that of the larger band gap material ($CuGaO_2$), the $CuGaO_2$/ZnO heterojunction can be considered as type II (staggered) heterojunction, whereas the band gap of ZnO is completely contained in the band gap of the ZnMgO, and hence ZnMgO/ZnO heterojunction can be considered as type I (straddling) heterojunction. From the band diagram, it is clear that in the asymmetric MQW, the holes will move to the $CuGaO_2$ side and electrons to the ZnO side. But in the symmetric MQW, both carriers will be confined in ZnO confinement layer itself. The thickness of the individual layers of the MQW was confirmed from the cross section images recorded using high resolution transmission electron microscopy (HRTEM). A representative HRTEM image of the asymmetric MQW structure having confinement layer (ZnO layer) thickness 2 nm is shown in Figure 2. It shows that the confinement layer has a thickness of 8 nm and the barrier layer have thickness of 16 nm. Thus there is a discrepancy in the thickness measured from the rate of growth and the actual thickness.

The crystallinity of thin films was analysed by X-ray diffraction (XRD) using Cu-K_α radiation ($\lambda = 1.5418$ Å). Photoluminescence (PL) measurements at

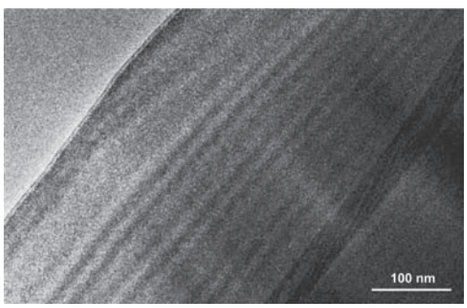

Figure 2. Cross sectional TEM image of the $CuGaO_2$/ZnO/ZnMgO asymmetric MQW grown by pulsed laser deposition.

room temperature were done by exciting the samples using the fourth harmonic of a Nd:YAG laser ($\lambda_{ex} = 266$ nm). Temperature dependence PL measurement of the MQWs was performed from 80 K up to room temperature using the 325-nm line of a He–Cd laser as the excitation source. The luminescence was analyzed through a Horiba Jobin Yvon LabRam spectrometer that was equipped with a Linkam cryostat.

3. RESULTS AND DISCUSSION

XRD pattern of the ZnO, $CuGaO_2$ thin films and the symmetric and asymmetric MQW are shown in Figure 3. In all the spectra, one can see a sharp peak at $2\theta = 41°$ that corresponds to the (0006) reflection from the sapphire substrate. The most intense contribution in the XRD pattern of ZnO thin film, $CuGaO_2$/ZnO/ZnMgO asymmetric and

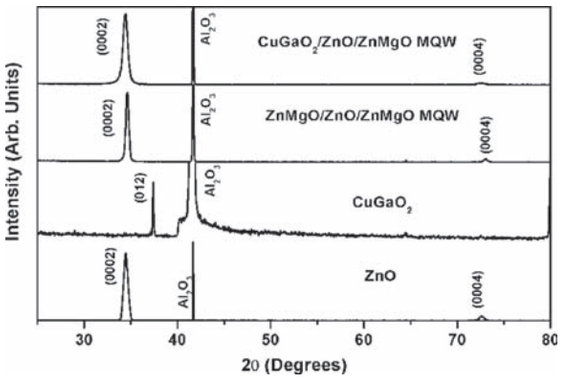

Figure 3. XRD pattern of ZnO thin film, $CuGaO_2$ thin film and $CuGaO_2$/ZnO/ZnMgO asymmetric and ZnMgO/ZnO/ZnMgO symmetric MQW grown on Al_2O_3 substrate.

ZnMgO/ZnO/ZnMgO symmetric MQW corresponds to the crystal plane of wurtzite ZnO along [0001] growth direction. The strong intensity of the (0002) reflection with narrow width also shows that the *c*-axis of ZnO is well oriented along the normal direction of the substrate surface. On the other hand, the (012) planes of $CuGaO_2$ identified from the XRD pattern confirm the formation of delafossite structure. The peaks of secondary phases, such as Cu_2O and $CuGa_2O_4$ were not detected in the XRD pattern.

Figure 4 shows the room temperature PL emission at an excitation wavelength of 266 nm from $CuGaO_2$/ZnO/ZnMgO asymmetric and ZnMgO/ZnO/ZnMgO symmetric MQWs with 2 nm confinement layer thickness. The spectra of a ZnO thin film having a thickness of 150 nm grown over Al_2O_3 substrate by PLD is also presented for comparison. Symmetric MQW shows a sharp PL emission centered at 361 nm corresponding to the band edge of ZnO. This PL peak has a FWHM of 20 nm suggesting that the MQW has good crystalline quality. The blue shift in the PL peak position with respect to the bulk is attributed to

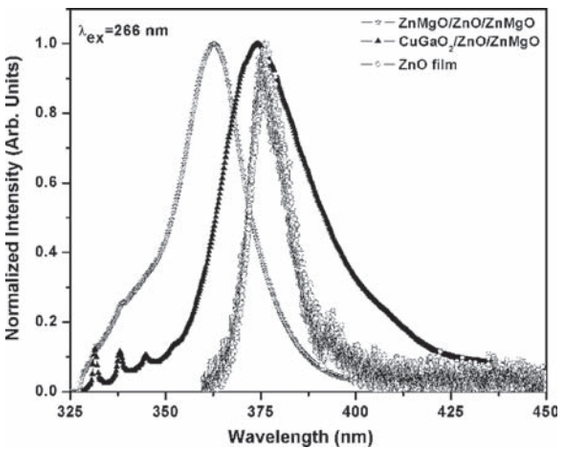

Figure 4. Normalized PL spectra from ZnO film, $CuGaO_2$/ZnO/ZnMgO asymmetric and ZnMgO/ZnO/ZnMgO symmetric MQW structures at room temperature.

the quantum confinement effects.[21] A shoulder at shorter wavelengths ($\approx$350 nm) is also presented in the spectrum that corresponds to the emission from the ZnMgO barrier layer.[22] The PL spectrum of the asymmetric MQW sample present a similar line shape but red-shifted due to the higher thickness of the confinement layer than calculated from the rate of growth.

Figures 5(a) and (b) show PL spectra from the symmetric and asymmetric MQW structures for two different thicknesses of ZnO confinement layer, 2 nm and 6 nm respectively. A blue shift in the PL peak position is clearly seen as the ZnO well thickness is varied from 6 nm to 2 nm as a consequence of an increase in the quantum confinement effect. Also, the FWHM of the PL bands increases with decreasing thickness of the confinement layer, which can be attributed to thickness fluctuations in well layer or to some roughness in the interface for thinner wells.

The infinite well approximation is the simplest method to calculate the quantum energy of carriers in the valance band well and the conduction band well. It is possible to evaluate the energy shift of the PL emission with respect to the one in bulk ZnO as a function of the well thickness, by considering the QW as an infinite well and following the expression

$$E_n = \frac{\hbar^2}{2m^*}\left[\frac{(n+1)\pi}{L_{QW}}\right]^2 \quad (1)$$

where m^* and L_{QW} are the effective mass of electron in bulk ZnO and the confinement layer thickness, respectively, while n is an integer that refers to the different excited states within the well (n equal to zero corresponds to the energy of the lowest energy state).[23]

Using this simple model, the confinement layer thickness of $CuGaO_2$/ZnO/ZnMgO asymmetric MQW structures estimated from the PL peak position was found to be larger than that estimated using the growth rates. The 2 nm thick confinement layer, as calculated from the rate of growth, has a thickness of 8 nm as observed from the TEM images. This is consistent with that calculated from the PL peak position. Consequently, due to the larger thickness of the confinement layer, relatively small blue shift in the PL peak positions with bulk was observed.

Similarly, the PL peak position revealed the ZnO confinement layer thickness as 4 nm for the symmetric MQW structures, whereas the estimated thickness from the rate of growth was 2 nm. Therefore, there is a discrepancy in the estimation of layer thickness values between these two methods. The small blue shift in the PL peak position for the higher active layer thickness in comparison with the bulk is attributed to the weak quantum confinement effects at larger confinement layer thicknesses. Similarly, using the same model, a confinement layer thickness of 10 nm was obtained for those symmetric MQW structures whose confinement layer thickness was expected to be 6 nm from the rate of growth. The larger thickness of

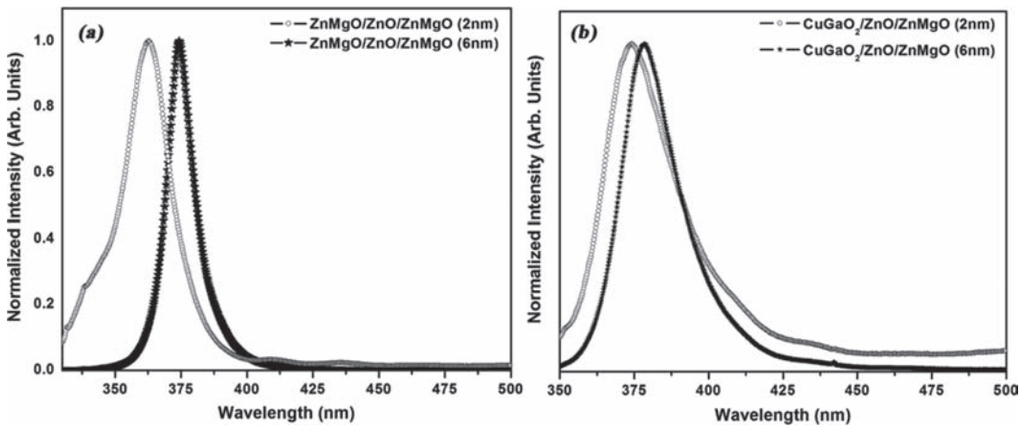

Figure 5. Room temperature PL emission from (a) ZnMgO/ZnO/ZnMgO symmetric and (b) $CuGaO_2$/ZnO/ZnMgO asymmetric MQWs for 2 nm and 6 nm of the ZnO confinement layer.

the confinement layer results in a small variation in the PL peak position from that of the bulk, since the quantum confinement is less prominent. The quantum confinement in nanostructures is only expected for structures with one dimension, whose sizes are comparable to the exciton Bohr radius. The exciton Bohr radius of ZnO is only ~ 2 nm.[24]

We have performed temperature dependence PL measurements on the symmetric and asymmetric MQW structures that presented larger electronic quantum confinement (i.e., thinner ZnO thickness). In Figures 6(a) and (b) we depicted the PL spectra of ZnMgO/ZnO/ZnMgO symmetric MQW having 2 nm thick confinement layers and $CuGaO_2$/ZnO/ZnMgO asymmetric MQW having 6 nm thick confinement layers for temperatures ranging from 80 K up to room temperature ($T = 294$ K). It can be observed that both the peak intensity and the integral intensity of the PL emission decrease with increase of temperature in MQWs. Thermal quenching of this emission line can be described by[25]

$$I(T) = \frac{I(T=0)}{1 + C\exp(-E_a/(KT))} \tag{2}$$

where $I(T)$ is the PL intensity at temperature T, C is the constant describing the capture of carriers at centre and E_a is the activation energy of the quenching process.

The values of integral intensity of the PL emission from the asymmetric and symmetric MQWs as a function of the temperature are shown in Figures 7(a) and (b). The experimental data was fitted with the theoretical equation given in 2 to calculate the activation energy of the carriers. The values of the activation energies for the asymmetric and symmetric structures were 32.71 meV and 24.6 meV respectively. The constant C for asymmetric and symmetric structures was 22.03 and 2.2×10^{10} respectively.

The variation of PL peak position of the symmetric and asymmetric MQWs with temperature is shown in Figure 7(c). The red shift in the PL peak position with increasing temperature is due to the temperature induced band gap shrinkage. The PL peak position corresponds to the symmetric MQWs is found to have higher energy than that of asymmetric MQWs grown by PLD. This is due to the lower thickness of ZnO confinement layer in symmetric MQW (2 nm) than the asymmetric MQW (6 nm).

Figure 7(d) shows the variation of the full width at half maximum (FWHM) of PL peak with temperature for

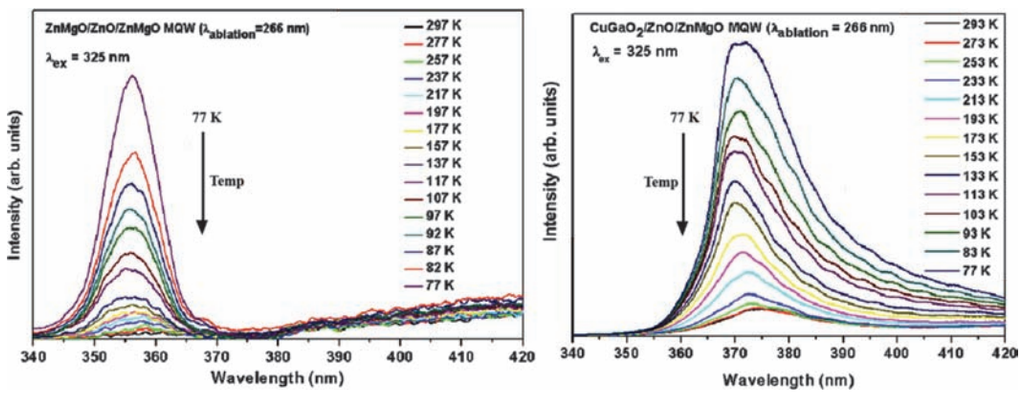

Figure 6. Low temperature PL of (a) symmetric ZnMgO/ZnO/ZnMgO MQW and (b) asymmetric $CuGaO_2$/ZnO/ZnMgO MQW.

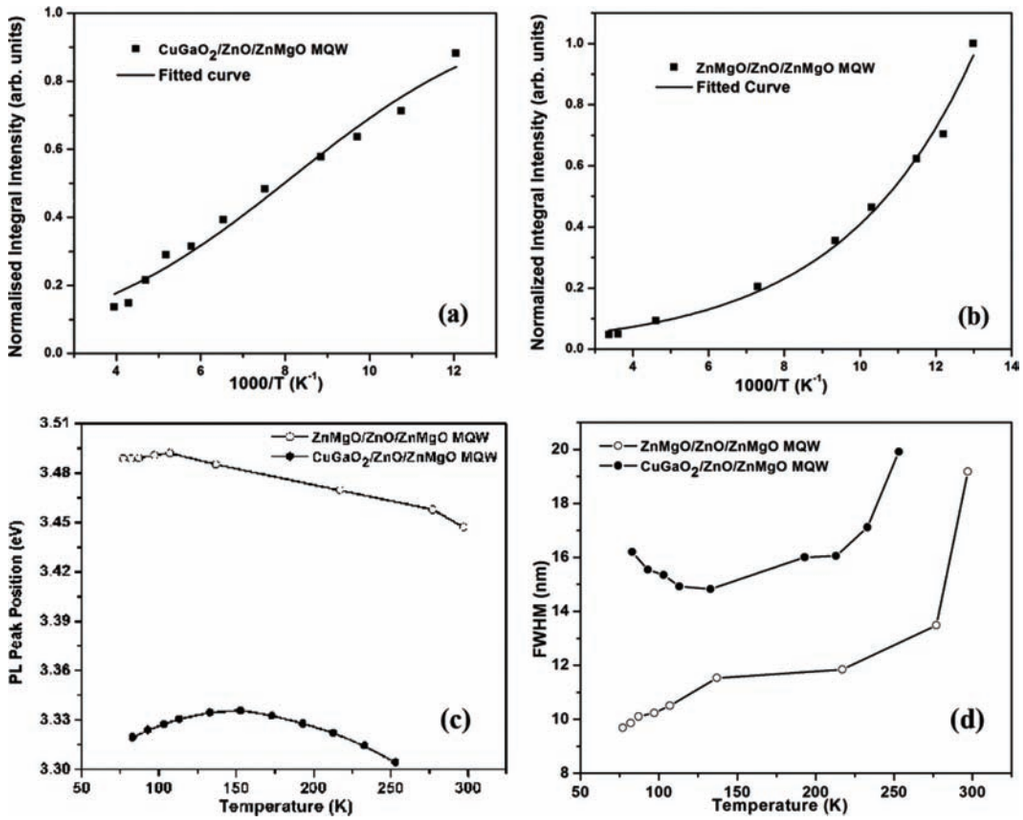

Figure 7. Variation with temperature of (a) and (b) PL integral intensity, (c) PL peak position (d) FWHM of PL peak of $CuGaO_2$/ZnO/ZnMgO asymmetric and ZnMgO/ZnO/ZnMgO symmetric MQWs.

symmetric and asymmetric MQWs. The FWHM of PL peaks is found to increase with temperature. Line width of PL peak of MQWs increases gradually up to 200 K and then exponentially up to RT. The linear increase in line width below 200 K implies the dominance of acoustic phonon scattering at lower temperatures.[26] Exponential increase in line width at higher temperature range indicates that the exciton-Longitudinal Optic (LO) phonon interaction predominates the PL line width.[27]

4. CONCLUSIONS

$CuGaO_2$/ZnO/ZnMgO asymmetric and ZnMgO/ZnO/ZnMgO symmetric multiple quantum well structures with varying confinement layer thickness were grown by buffer assisted pulsed laser deposition using the fourth harmonic of a Nd:YAG laser. Efficient room temperature photoluminescence emission was observed from the asymmetric and symmetric MQW structures and temperature dependence on the PL peak position, FWHM and integral intensity of emission from asymmetric and symmetric MQWs were studied. The PL emission of asymmetric and symmetric MQW structures was blue shifted with a decrease in the confinement layer thickness from 6 to 2 nm, which is attributed to quantum confinement effects. The PL emission from asymmetric and symmetric MQW structures is blue shifted compared to that of 150 nm thick ZnO thin film. The thickness of the confinement layer estimated from the rate of deposition and from PL peak positions are not in agreement. A more accurate in-situ method is required to have precise control of the confinement layer thickness.

Acknowledgments: The work was supported by the Department of Science and Technology, Government of India under Nanoscience and Technology Initiative. The authors (P. M. Aneesh) thank the Council of Scientific and Industrial Research for the award of research fellowship.

References and Notes

1. T. Makino, Y. Segawa, M. Kawasaki, and H. Koinuma, *Semicond. Sci. Technol*. 20, S78 **(2005)**.
2. H. D. Sun, T. Makino, N. T. Tuan, Y. Segawa, Z. K. Tang, G. K. L. Wong, M. Kawasaki, A. Ohtomo, K. Tamura, and H. Koinuma, *Appl. Phys. Lett*. 77, 4250 **(2000)**.
3. H. D. Sun, T. Makino, Y. Segawa, M. Kawasaki, A. Ohtomo, K. Tamura, and H. Koinuma, *J. Appl. Phys*. 91, 1993 **(2002)**.
4. U. Ozgur, Y. I. Alivov, A. Teke, C. Liu, M. A. Reshchikov, S. Dogan, V. Avrutin, S. J. Cho, and H. Morkoc, *J. Appl. Phys*. 98, 041301 **(2005)**.
5. P. Misra, T. K. Sharma, S. Porwal, and L. M. Kukreja, *Appl. Phys. Lett*. 89, 161912 **(2006)**.

6. T. Gruber, C. Kirchner, R. Kling, and F. Reuss, *Appl. Phys. Lett*. 84, 5359 **(2004)**.
7. A. Ohtomo, M. Kawasaki, I. Ohkubo, H. Kojinuma, T. Yasuda, and Y. Segawa, *Appl. Phys. Lett*. 75, 980 **(1999)**.
8. T. Makino, C. H. Chia, Nguen T. Tuan, H. D. Sun, Y. Segawa, M. Kawasaki, A. Ohtomo, K. Tamura, and H. Koinuma, *Appl. Phys. Lett*. 77, 975 **(2000)**.
9. B. P. Zhang, N. T. Binh, K. Wakatsuki, C. Y. Liu, Y. Segawa, and N. Usami, *Appl. Phys. Lett*. 86, 032105 **(2005)**.
10. A. Ohtomo and A. Tsukazaki, *Semicond. Sci. Technol*. 20, S1 **(2005)**.
11. S. Krishnamoorthy, A. A. Iliadis, A. Inumpudi, S. Choopun, R. D. Vispute, and T. Venkatesan, *Solid-State Electron*. 46, 1633 **(2002)**.
12. T. Makino, N. T. Tuan, H. D. Sun, C. H. Chia, Y. Segawa, M. Kawasaki, A. Ohtomo, K. Tamura, T. Suemoto, H. Akiyama, M. Baba, S. Saito, T. Tomita, and H. Koinuma, *Appl. Phys. Lett*. 78, 1979 **(2001)**.
13. H. D. Sun, T. Makino, N. T. Tuan, Y. Segawa, M. Kawasaki, A. Ohtomo, K. Tamura, and H. Koinuma, *Appl. Phys. Lett*. 78, 2464 **(2001)**.
14. S. Ikeda, A. Shimizu, and T. Hara, *Appl. Phys. Lett*. 55, 1155 **(1989)**.
15. C. Juang, K. J. Kuhn, and R. B. Darling, *IEEE J. Quantum Electronics* 27, 2122 **(1991)**.
16. T. Tsuchiya, S. Katayama, and T. Ando, *Surf. Sci.* 361/362, 376 **(1996)**.
17. K. Ueda, T. Hase, H. Yanagi, H. Kawazoe, H. Hosono, H. Ohta, M. Orita, and M. Hirano, *J. Appl. Phys*. 89, 1790 **(2001)**.
18. H. Kawazoe, M. Yasukawa, H. Hyodo, M. Kurita, H. Yanagi, and H. Hosono, *Nature* 389, 939 **(1997)**.
19. V. Varadarajan and D. P. Norton, *Appl. Phys. A* 85, 117 **(2006)**.
20. X. Nie, S. H. Wei, and S. B. Zhang, *Phys. Rev. Lett.* 88, 66405 **(2002)**.
21. K. F. Lin, H. M. Cheng, H. C. Hsu, L. J. Lin, and W. F. Hsieh, *Chem. Phys. Lett*. 409, 208 **(2005)**.
22. J. Zhu, A. Y. Kuznetsov, M. S. Han, Y. S. Park, H. K. Ahn, J. W. Ju, and I. H. Lee, *Appl. Phys. Lett*. 90, 211909 **(2007)**.
23. J. H. Davies, The Physics of Low-Dimensional Semiconductors: An Introduction, 6th Reprint edn., Cambridge University Press, New York, USA **(2006)**.
24. R. T. Senger and K. K. Bajaj, *Phys. Rev. B* 68, 045313 **(2003)**.
25. J. P. Dean, *Phys. Rev.* 157, 655 **(1967)**.
26. R. Hellmann, M. Koch, J. Feldmann, S. T. Condiff, E. O. Gobel, D. R. Yakovlev, A. Waag, and G. Landwehr, *Phys. Rev. B* 48, 2847 **(1993)**.
27. M. O'Neill, M. Oestreich, W. W. Ruhle, and D. E. Ashenford, *Phys. Rev. B* 48, 8980 **(1993)**.

Received: 31 March 2013. Accepted: 29 December 2013.